Slow shocks and particle heating in impulsive solar flares

H. Arnold[1], J. F. Drake[1] , M. Swisdak[1], J. Dahlin[2], F. Guo[3], J. Karpen[2], C. R. DeVore[2], S. Antiochos[2]

SolFER Meeting 2021

1. Abstract

- Solar flares both heat plasma[1] and accelerate particles to nonthermal energies[2]
- This process is not well understood. We present a new a mechanism that can contribute to the energy gain of the plasma in magnetic reconnection
- Recent macro-scale kinetic simulations with the new code *kglobal*[3,4] have led to the discovery of the generation of large numbers of slow shocks upstream of the reconnecting current layer[5,6]
- As magnetic islands grow and merge together they create fast flows in the upstream region as plasma moves to fill in the low-pressure regions created by the plasmoid motion
- These flows steepen into slow shocks that heat the plasma upstream
- These shocks have been observed in MHD simulation[5,6] and global simulations of CMEs with the ARMS code[7] and
- As the CME is ejected, Alfvénic downflows lead to the formation of slow shocks

2. Slow Shocks

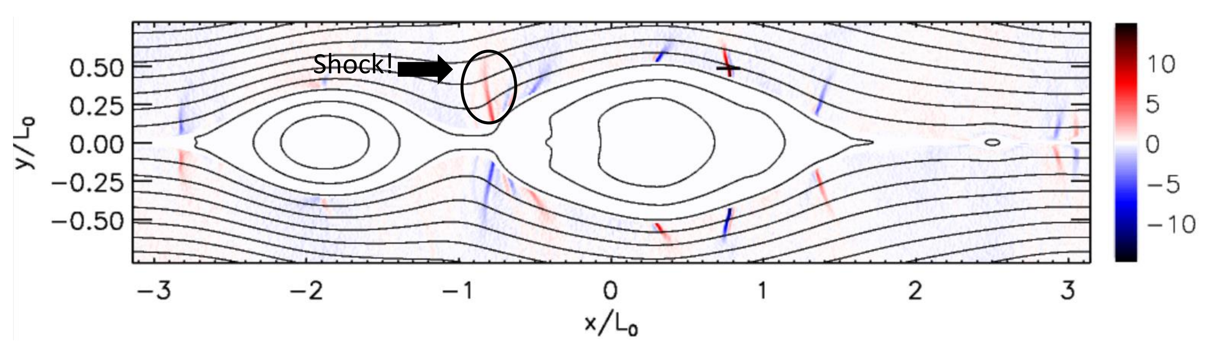

Fig. 1. $\mathbf{b}\cdot\nabla n$ outside the separatrix for a simulation with B_g/B_0=0.6 and β_r=0.5. The solid line at y=0.5 and 0.7<x<.85 corresponds to the cuts in Fig.2

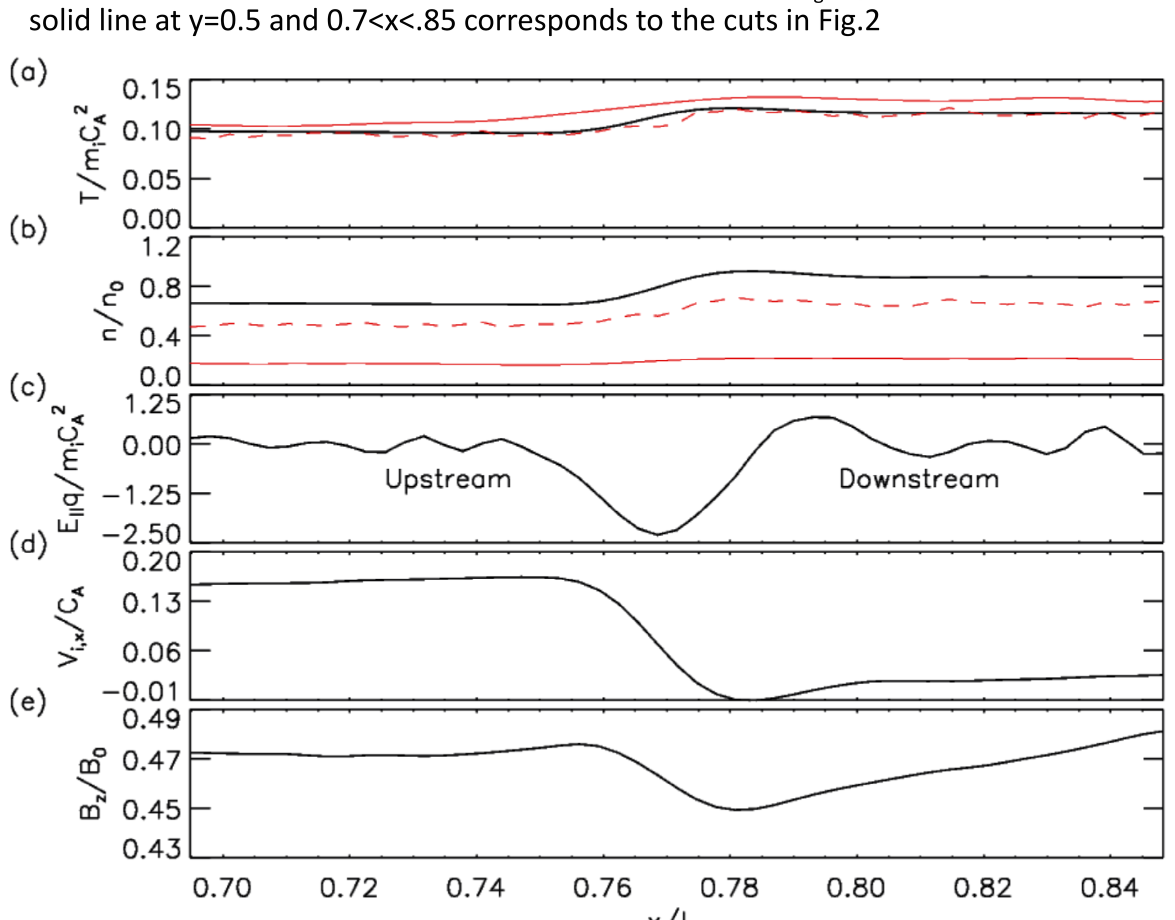

Fig. 2. Cuts across a slow shock of (a) ion, electron fluid, and electron particle temperatures, (b) densities, (c) the parallel electric field, (d) the normal flow velocity, and (e) the guide field.

- Slow Shocks show compression, plasma heating, and an out of phase shift of the guide field
- The kglobal code includes an $E_{\|}$ that other macro-scale simulations do not[4]
  - $E_{\|} = -\frac{1}{en_i}\mathbf{b}\cdot\nabla\cdot\overline{\overline{\mathbf{P}}}_e$

0. Authors

[1] University of Maryland, College Park, MD
[2] NASA Goddard Space Flight Center, Greenbelt, MD
[3] Los Alamos National Lab, Los Alamos, NM

3. Slow Shock Formation

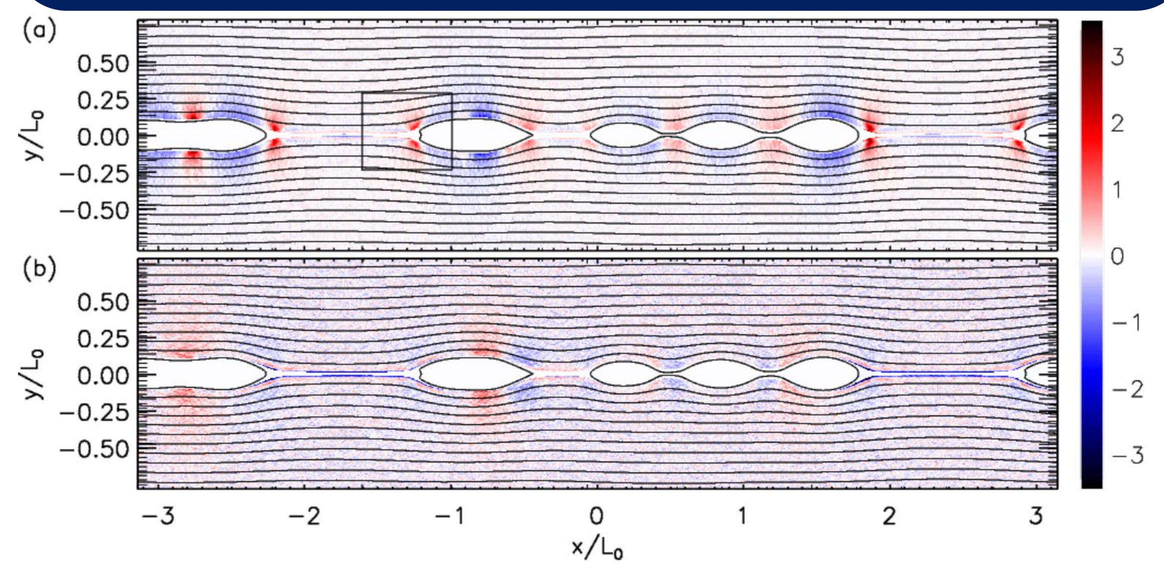

Fig. 3. (a) $\nabla\cdot nv_{\|}$ (b) $\nabla\cdot nv_{\perp}$. The box in (a) corresponds to the region shown in Fig. 4

- Plasma compression is from parallel flows

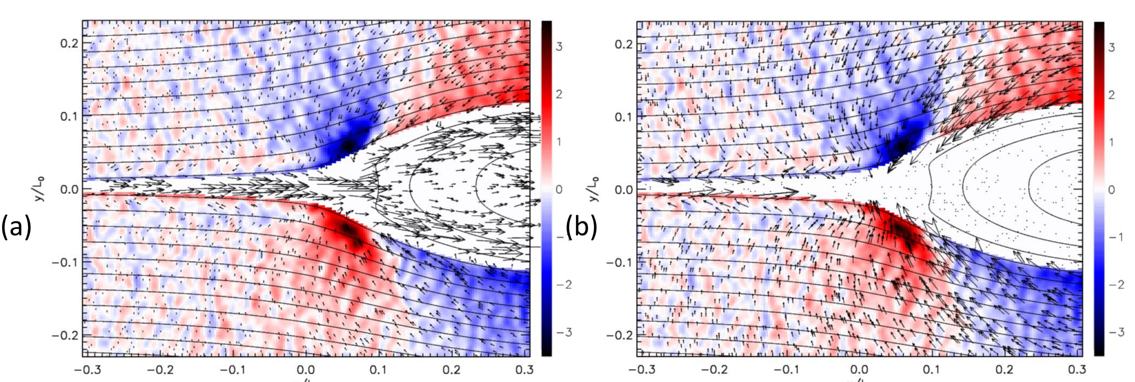

Fig. 4. (a) $\mathbf{b}\cdot\nabla n$ with arrows showing in plane flow (b) $\mathbf{b}\cdot\nabla n$ with the flow in the separatrix zeroed out to emphasize upstream flows.

- The island in Fig. 4 is moving to the right causing flows to fill in the region behind.
- These flows create a divergence in the parallel ion flux leading to compression and eventually steepening into slow shocks
- The following equation shows the drivers of the parallel ion flux ($\boldsymbol{\kappa}$ is the magnetic curvature and $\overline{\overline{P}}$ is a tensor including the ion and electron pressures):

Eqn 1.
$$\frac{\partial m_i n_i v_{i,\|}}{\partial t} = \frac{m_i n_i}{2}\hat{\boldsymbol{b}}\cdot\nabla v_{i,\perp}^2 - \nabla\cdot m_i n_i \vec{v}_i v_{i,\|} + m_i n_i v_{i,\|}\vec{v}_{i,\perp}\cdot\vec{\boldsymbol{\kappa}} - \hat{\boldsymbol{b}}\cdot\nabla\cdot\overline{\overline{\boldsymbol{P}}}$$

- The first and last terms on the RHS can drive the parallel flow
- A high guide field can suppress the formation of the slow shocks by decreasing the strength of the parallel flow drivers

4. Varying the Guide Field

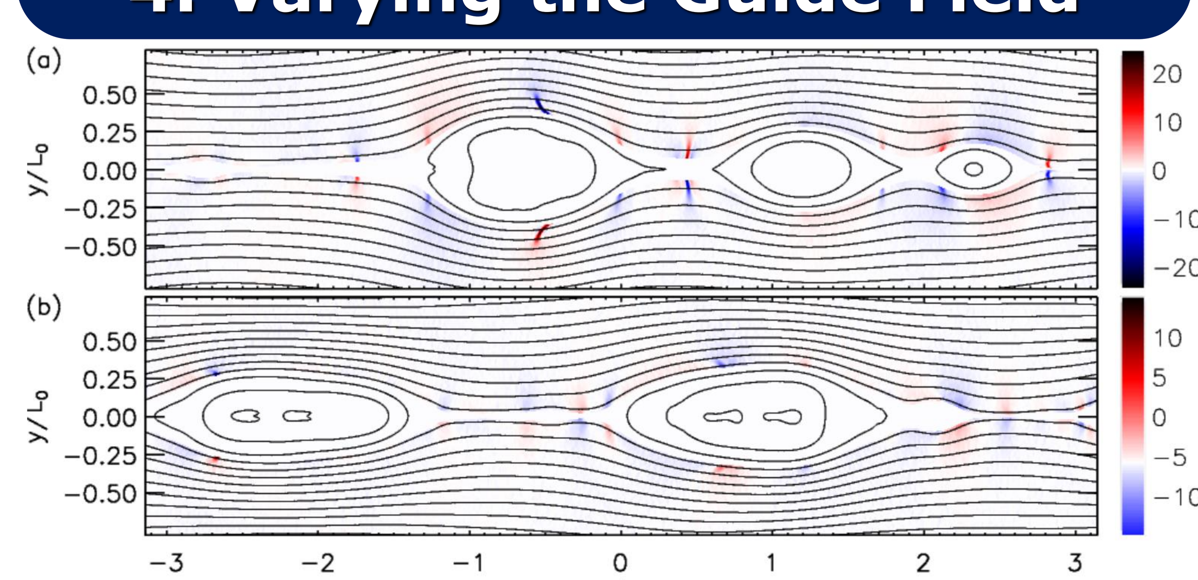

Fig. 5. $\mathbf{b}\cdot\nabla n$ for simulations with β_r = 0.125 and B_g/B_0 = (a) 0.6 and (b) 1.0

- High guide field simulations still show slow shock like features, however they are:
  - smaller in magnitude,
  - spatially more spread out, and
  - do not extend as far upstream.

5. Varying β_r

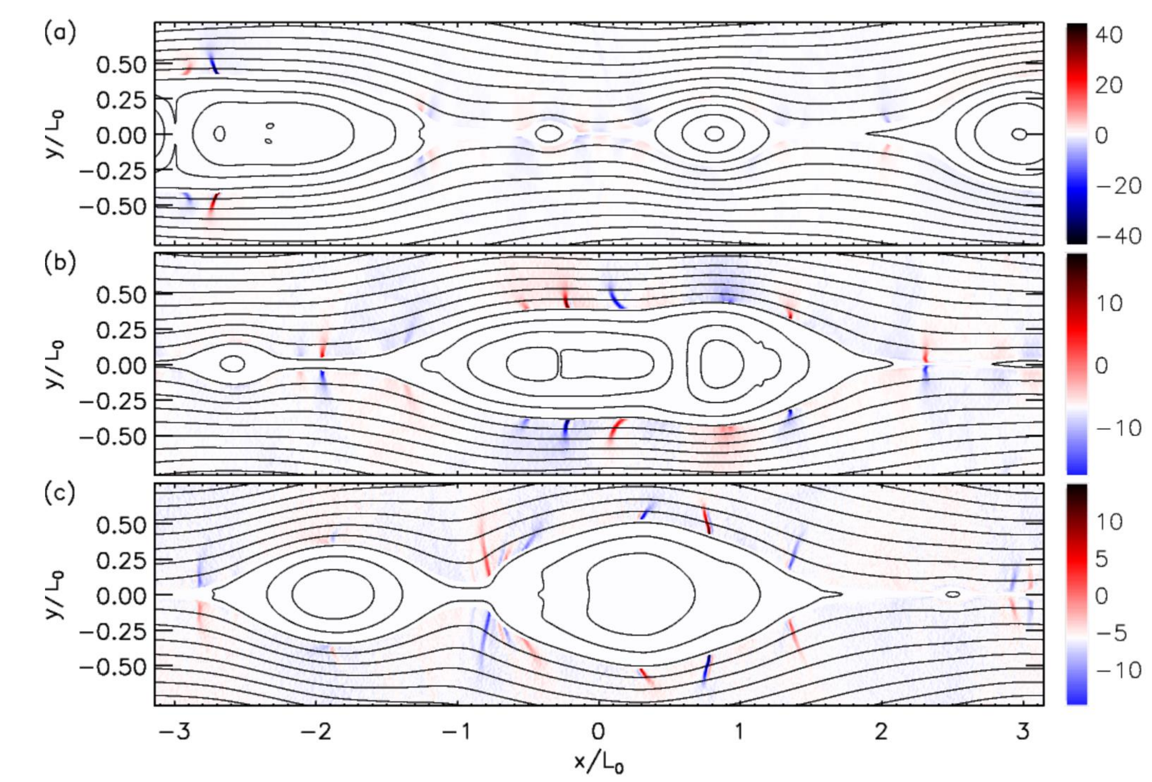

Fig. 6. $\mathbf{b}\cdot\nabla n$ for simulations with B_g/B_0 = 0.6 and β_r = (a) 0.0625, (b) 0.125 and (c) 0.5

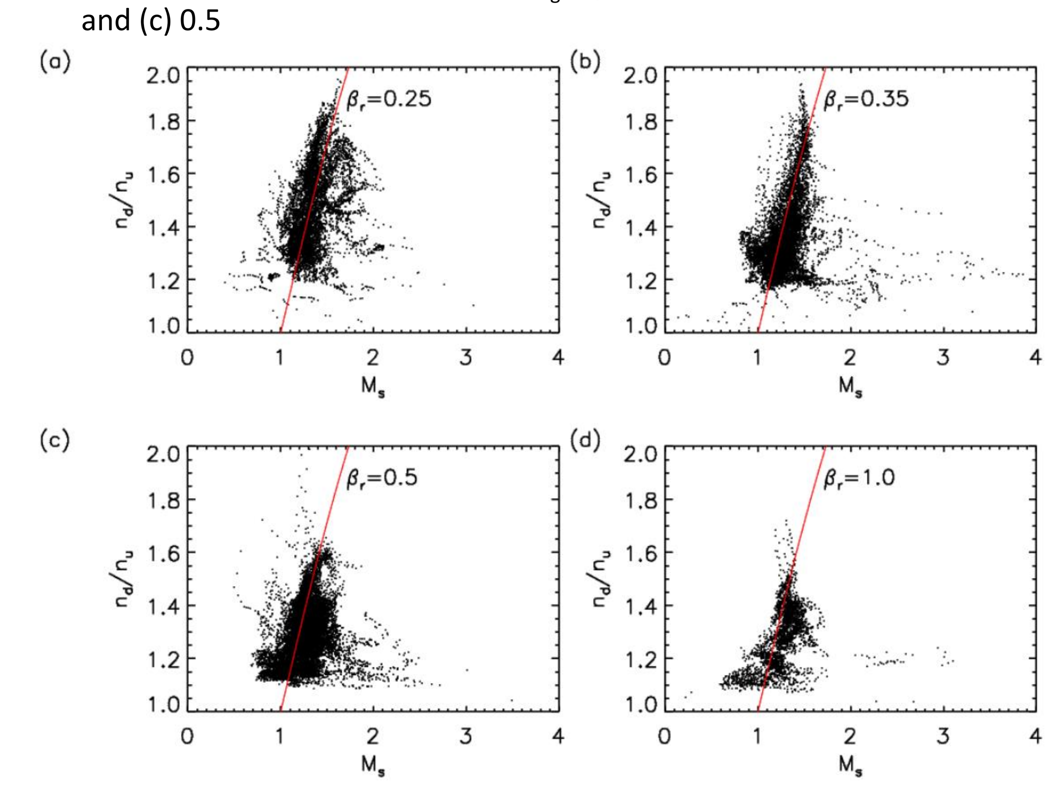

Fig. 7. Scatter plots of the compression ratio vs the sonic Mach number at multiple points across shocks throughout the duration of the simulation for B_g/B_0 = 0.25 and β_r = (a) 0.25, (b) 0.35, (c) 0.5 and (d) 1.0

- Simulations show slow shock formation at large and small plasma β_r
- Shocks at smaller plasma β_r tend to be stronger due to the reduction in the slow speed. The last term in Eqn. 1 is reduced at small β_r, but the first term is unchanged
- Fig. 7 includes red lines that show the slow shock relationship:

$$n_d/n_u = 4M_s^2/(M_s^2 + 3)$$

6. Global Simulations of CMEs

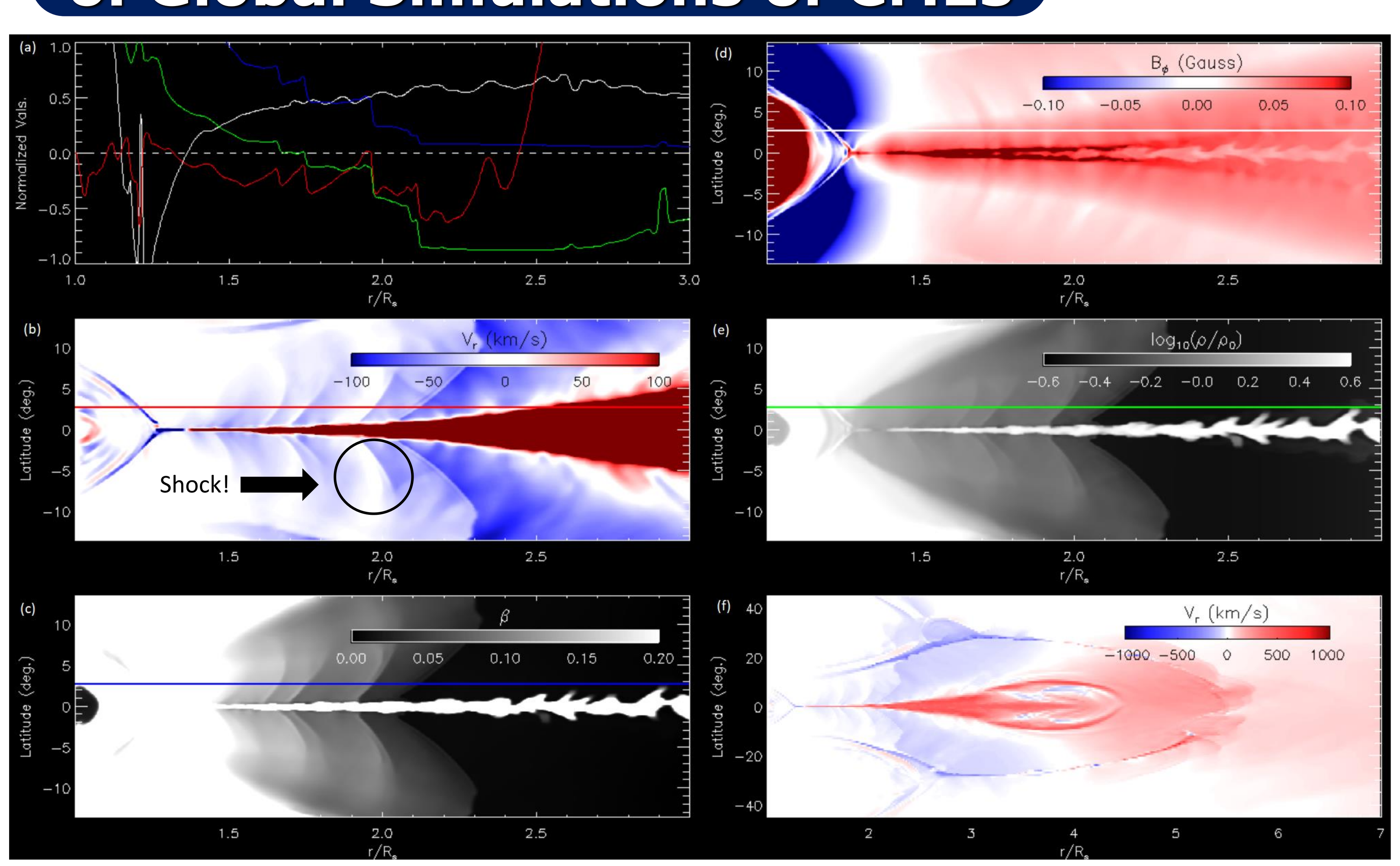

Fig. 8. Results of a global simulation of a CME with the ARMS code. Panels b-e are zoomed in around the flaring reconnecting sheet. (a) shows cuts along the horizontal lines in other panels. (b) The radial velocity. (c) the plasma β. (d) The out of plane (or guide) field. (e) log of the plasma density. (f) a global view of the radial velocity. Note that all panels are overexposed to show slow shocks

- As the CME is ejected, downflows are formed behind the CME that steepen into shocks just as before
- Panel (a) shows the out of phase relationship between the guide field and the density jump, a key indicator of slow shocks
- Panel (f) illustrates that the size of the slow shocks scale like the CME size

7. Conclusion

- Large scale slow shocks that extend far upstream of the separatrix are formed in multi island magnetic reconnection as a result of plasmoid motion
- A large guide field suppresses the formation of the slow shocks
- These slow shocks may play a role in heating the plasma in solar flares and other magnetic reconnection scenarios
- See companion movie for a movie of the slow shocks. Top panel is $v_{i,x}$, middle panel is $v_{i,y}$, and bottom is $\mathbf{b}\cdot\nabla n$

8. References

[1] Aschwanden, M., Boerner, P., Ryan, D., Amir, C., McTiernan, J., and Warren, H. (2015) Global Energetics of Solar Flares. II. Thermal Energies, *The Astrophysical Journal*, **802**, 53 doi: 10.1088/0004-637X/802/1/53

[2] Aschwanden, M., Holman, G., O'Flannagain, A., Amir, C., McTiernan, J., and Kontar, E. (2016) Global Energetics of Solar Flares. III. Nonthermal Energies, *The Astrophysical Journal*, **832**, 27, doi: 10.3847/0004-637X/832/1/27

[3] Drake, J. F., Arnold, H., Swisdak, M., Dahlin, J. T. (2019) A computational model for exploring particle acceleration during reconnection in macroscale systems, *Physics of Plasmas*, **26**, 012901, doi: 10.1063/1.5058140

[4] Arnold, H., Drake, J. F., Swisdak, M., Dahlin, J. T. (2019) Large-Scale Parallel Electric Fields and Return Currents in a Global Simulation Model, *Physics Of Plasmas*, **26**, 102903, doi:10.1063/1.5120373

[5] Zenitani, S., and Miyoshi, T. (2011) Magnetohydrodynamic structure of a plasmoid in fast reconnection in low-beta plasmas, *Physics of Plasmas*, **18**, 022105, doi:10.1063/1.3554655

[6] Zenitani, S., and Miyoshi, T. (2020) Plasmoid-dominated Turbulent Reconnection in a Low-β Plasma, *The Astrophysical Journal Letters*, **894**, L7, doi:10.3847/2041-8213/ab8b5d

[7] Karpen, J. , Antiochos, S., and DeVore, C. (2012) The Mechanisms for the Onset and Explosive Eruption of Cornoal Mass Ejections and Eruptive Flares, *The Astrophysical Journal*, **760**, 81, doi:10.1088/0004-637X/760/1/81